Research Square

Preprints are preliminary reports that have not undergone peer review.
They should not be considered conclusive, used to inform clinical practice,
or referenced by the media as validated information.

Multi-Decadal Analysis of Channel Migration and Morphological Transition of the Padma River Using Landsat Satellite Imagery

Milon Bokshi

mbokshi45@gmail.com

Institute of Water Modelling

Md. Nurul Islam

Jahangirnagar University

Md. Munir Mahmud

Jahangirnagar University

Md. Jakir Hossain

Jahangirnagar University

Research Article

Keywords: Padma River, Channel Migration, Landsat, Geospatial Analysis, Bengal Delta

Posted Date: November 26th, 2026

DOI: https://doi.org/10.21203/rs.3.rs-11493747/v1

License: This work is licensed under a Creative Commons Attribution 4.0 International License. Read Full License

Additional Declarations: No competing interests reported.

Abstract

This study examines the long-term morphodynamic evolution of the Padma River, one of the most morphologically unstable channels in the Bengal Delta system, between 1988 and 2026 using multi-temporal Landsat imagery and geospatial morphometric analysis. The river was segmented into five distinct reaches. Segment-wise analyses of sinuosity, Aerial Braided Index (ABI), and channel migration were conducted to quantify long-term morphodynamic behavior and planform evolution. Results reveal substantial lateral migration, braided expansion, meander adjustment, and repeated channel reorganization throughout the study period. Temporal variations in sinuosity and ABI exhibit quasi-cyclic oscillatory behavior, suggesting a dominant morphodynamic cycle of approximately 12–18 years with shorter sub-cycles of 6–8 years. Despite cyclic fluctuations, the long-term increase in ABI indicates progressive enhancement of braided instability and sediment redistribution. Segment-wise variations further suggest possible localized downstream influences. These findings provide insights into the long-term instability and evolutionary behavior of the Padma River, emphasizing the need for continuous geomorphological monitoring and sustainable river management strategies in the Bengal Delta region.

1. Introduction

Large alluvial rivers are inherently dynamic systems characterized by continuous adjustment of channel geometry, planform configuration, sediment transport, and bank-line position. These morphological changes are primarily controlled by variations in discharge, sediment supply, channel slope, bank material composition, and anthropogenic interventions (Wolman & Leopold, 1957; Schumm, 1985). Rivers within the Ganges–Brahmaputra–Meghna (GBM) basin are among the most morphologically active fluvial systems in the world due to their enormous sediment load and highly seasonal monsoonal hydrology (Goodbred & Kuehl, 2000). The GBM river system carries an estimated 1–1.25 billion tonnes of sediment into the Bengal Delta every year (Rahman et al., 2018). The combined sediment load specifically carried by the Ganges and Brahmaputra rivers is approximately 1 billion tonnes per year (Islam et al., 1999). Among these, the Padma River, the principal distributary of the Ganges and the Brahmaputra within Bangladesh, exhibits significant channel migration, braiding, erosion, and bar formation, making it one of the most unstable large rivers in South Asia (Dewan et al., 2017; Preota et al., 2026). The Padma in particular, trustworthy sources generally state a mean discharge of about 30,000 m^3/s, a bank-full discharge of approximately 75,000 to 80,000 m^3/s (Miah et al., 2025; Islam et al., 2022).

Variability in discharge regime and sediment transport promotes continuous alternation between channel widening, narrowing, bifurcation, and realignment. Such dynamic rivers often exhibit oscillatory or quasi-cyclic morphological behavior characterized by alternating phases of increased sinuosity, enhanced braiding, and channel stabilization (Wahiduzzaman & Yeasmin, 2022). Understanding these long-term morphodynamic patterns is essential for river management, erosion mitigation, infrastructure planning, and hazard assessment in Bangladesh.

However, its unstable morphology causes extensive riverbank erosion, floodplain reworking, agricultural land loss, and displacement of riverside populations every year (Ophra et al., 2018). The river continuously

modifies its channel through lateral migration, avulsion, formation and destruction of chars (mid-channel sandbars), and shifting of dominant flow pathways. Previous studies have investigated bank erosion and channel shifting of the Padma River using remote sensing and GIS techniques (Li et al., 2024; Chakraborty & Saha, 2022; Halder & Chowdhury, 2023). Nevertheless, comprehensive long-term analyses integrating sinuosity, braided intensity, and migration dynamics at a segment scale remain limited, particularly for studies extending into the most recent decade.

Recent advances in geospatial technologies and satellite remote sensing have enabled continuous monitoring of river morphodynamics over large spatial and temporal scales. Landsat satellite imagery, with its long historical archive and moderate spatial resolution, has become one of the most widely used datasets for fluvial geomorphological investigations (Zhao, et al., 2026; Hu et al., 2025; Li et al., 2014; Baki & Gan, 2012). Multi-temporal Landsat observations allow detailed assessment of river planform adjustment, channel migration, and temporal evolution of braided systems. Water-body extraction techniques based on spectral indices further improve the delineation of active river channels (Zaman et al., 2026; Hong et al., 2026). Among these techniques, the Normalized Difference Water Index (NDWI), proposed by McFeeters (1996), is extensively used to separate water and non-water features using green and near-infrared spectral bands. NDWI-based classification has proven effective for identifying active flow channels and exposed sediment bars in braided river environments (Marcus & Fonstad, 2008; Zhang et al., 2021).

This study investigates the long-term morphological evolution of approximately 105 km of the Padma River extending from the Jamuna–Padma confluence near Paturia to Chandpur Puran Bazar over the period 1988–2026. The resulting spatial patterns indicate substantial temporal and segment-wise variability in river morphology. Historical river-plane overlays reveal progressive outward expansion of the active channel corridor in several reaches, suggesting persistent lateral migration and reoccupation of floodplain areas. By integrating sinuosity, braided intensity, and migration analysis over nearly four decades, the research contributes to improved understanding of long-term river behavior in one of the world's most dynamic alluvial systems.

2. Methodology

2.1 Study Area

The study was conducted along approximately 105 km of the Padma River in central Bangladesh, extending from the confluence of the Ganges and Jamuna (Brahmaputra) Rivers near Paturia—where after merging with the Jamuna, the river is named the Padma—to Chandpur Puran Bazar, where the Padma joins the Meghna River, outstretched from 23.780° N, 89.795° E to 23.230° N, 90.628° E. before flowing toward the Bay of Bengal (Fig. 1). The study reach represents one of the most morphologically dynamic sections of the Ganges–Brahmaputra–Meghna (GBM) river system and is characterized by intense channel migration, braiding, bank erosion, and bar formation. Due to high seasonal discharge and sediment supply from the upstream, the river undergoes continuous planform adjustment and floodplain reworking. For geomorphological analysis, the river was subdivided into five segments (A–E) based on channel curvature, bend transition, and centerline density characteristics.

2.2 Satellite Data Collection and Preprocessing

Multi-temporal Landsat satellite imagery was used to analyze long-term river morphological changes between 1988 and 2026. Images were acquired from the United States Geological Survey (USGS) Landsat archive through the Google Earth Engine (GEE) cloud computing platform. To minimize the influence of seasonal hydrological variability, all images were selected from the dry-season low-flow period between December and February.

Images with cloud coverage greater than 10% were excluded to ensure reliable water-body extraction and channel delineation. In cases where suitable imagery was unavailable for a target year, the temporally nearest cloud-free image was selected. Thus, each analyzed year represents imagery acquired during December of the preceding year to February of the corresponding year. Different Landsat sensors were used depending on temporal availability, including Landsat 5 TM, Landsat 8 OLI, and Landsat 9 OLI-2.

2.3 Water-Land Classification, Delineating Braided Plane and Centerline Extraction

Water-body extraction was performed using the Normalized Difference Water Index (NDWI) proposed by McFeeters (1996). NDWI enhances water features by utilizing the spectral contrast between green and near-infrared (NIR) bands and is expressed as:

$$NDWI = \frac{Green - NIR}{Green + NIR}$$

1

Where, Green represents the reflectance of the green spectral band, and NIR represents the reflectance of the near-infrared spectral band. The NDWI was calculated within the Google Earth Engine environment for each temporal interval. Positive NDWI values (> 0) were classified as water bodies, while negative values represented non-water surfaces. The maximum active river plane or valley extent was manually digitized using the NDWI for all temporal intervals using ArcGIS. Within the active river plane water bodies (NDWI > 0) represent active flow channels, land represents exposed chars and sandbars located within the active channel belt (Du et al., 2016; Boothroyd et al., 2021).

For each analyzed year, a river centerline representing the dominant flow pathway was manually generated following the principal active channel. Centerlines were digitized within the active water channel to maintain consistency over the years. In braided reaches containing multiple channels, the centerline was positioned along the dominant conveyance pathway representing the primary river flow direction. The entire study reach was divided into five geomorphologically distinct segments (A–E). Segmentation was based on (1) changes in channel curvature, (2) transition between major bends, (3) line-density distribution of historical centerlines, and (4) termination points of meander-like half-circle structures. This segmentation framework allowed detailed reach-scale analysis of morphodynamic variability instead of treating the entire river as a homogeneous system.

2.4 Analysis of River Morphodynamics

Sinuosity was calculated for each river segment and temporal interval to quantify channel curvature and meandering intensity. Sinuosity was computed as the ratio between actual channel length and valley length where, sinuosity index (S), channel centerline length (L_c), and straight valley length (L_v) are correlated as below.

$$\mathrm{S} = \frac{L_c}{L_v}$$

2

Higher sinuosity values indicate increased meandering characteristics, whereas lower values represent straighter channel configurations (Bristow & Best, 1993; Islam & Guchhait, 2024). Temporal changes in sinuosity were analyzed to identify oscillatory behavior, long-term trends, and segment-wise morphological adjustment.

Braiding intensity was quantified using the Aerial Braided Index (ABI), which measures the proportion of bar area within the active river corridor. ABI was calculated segment-wise for each temporal interval following classification of water and exposed bar surfaces. The ABI is calculated using the area occupied by exposed bars/chars (A_b) and total active river area (A_r) and expressed in Eq. (3).

$$ABI = \frac{A_b}{A_r}$$

3

Higher ABI values indicate stronger braided characteristics associated with multiple channel threads and extensive sediment deposition (Yang et al., 2015; Arefin et al., 2021). Temporal ABI variations were examined to evaluate changes in braided intensity and channel instability throughout the study period.

Channel migration was analyzed using sequential two-year temporal intervals; for each interval, observation transects were generated at 1 km spacing from the earlier-year centerline toward the subsequent-year centerline. Migration distance was measured as the lateral displacement between corresponding centerline positions. Directional migration was categorized as leftward, and rightward migration. Figure 2 illustrates the methodological processes used in this study.

3. Results

The multi-temporal Landsat analysis between 1988 and 2026 reveals substantial long-term morphodynamic adjustment within the Padma River system. The analysis of historical river planes and centerlines demonstrates continuous channel reorganization through lateral migration, bar development, channel bifurcation, and alternating meandering–braiding behavior. The maximum river-plane analysis further demonstrates that the active river corridor has expanded considerably through time in braided reaches.

Areas characterized by multiple overlapping channel occupations correspond to zones of high channel instability and repeated avulsion. Conversely, relatively narrow overlap zones indicate comparatively stable reaches with constrained migration.

3.1 Meandering Characteristics and Temporal Evolution

The overall sinuosity (**Fig. 3**) of the Padma River varied between 1.046 and 1.206 during the study period, with a mean value of approximately 1.117. These values indicate that the study reach maintained a transitional morphology between low-sinuosity meandering and braided channel behavior throughout the analyzed period. The temporal sinuosity pattern exhibits clear oscillatory behavior rather than a monotonic increase or decrease. Initial sinuosity increased from 1.140 in 1988 to 1.204 in 1990, followed by fluctuations throughout the 1990s and early 2000s. A secondary increase occurred after 2010, before a gradual decline in later years. The resulting trend resembles a broad sinusoidal oscillation, indicating alternating phases of channel straightening and increased meandering.

a.

Figure 3 Sinuosity of the Padma River; (a) the overall sinuosity along the entire 105 km study reach from Paturia to Chandpur during 1988–2026; (b) Segment-wise sinuosity for the five geomorphological reaches (Segments A–E) over the same study period.

Segment A maintained relatively stable sinuosity (mean = 1.082) despite substantial channel shifting, suggesting that braided expansion and channel widening were the dominant adjustment mechanisms rather than enhanced meandering. In contrast, Segment B exhibited one of the largest fluctuations in sinuosity (mean = 1.107), with pronounced meander development during the early-to-mid 1990s followed by a decline, indicating episodic bend elongation, partial cutoffs, and subsequent channel simplification. Segment C showed a gradual increase in sinuosity after 2000 (mean = 1.063), coinciding with increasing ABI and broader channel occupation, suggesting a transition from a relatively stable reach to a more dynamic braided–meandering system. Although Segment D experienced considerable lateral channel translation, its sinuosity remained comparatively moderate (mean = 1.079), indicating that channel adjustment primarily occurred through lateral migration rather than increased meander curvature. Among all reaches, Segment E displayed the highest sinuosity variability (mean = 1.195), with values peaking at 1.681 during the late 1980s and early 1990s before declining, reflecting repeated phases of meander amplification, channel realignment, and possible cutoff formation. Collectively, these results demonstrate that the upstream reaches (Segments A–C) are predominantly characterized by braided channel expansion and gradual planform adjustment, whereas the downstream reaches, particularly Segment E, exhibit stronger meander-driven instability and oscillatory channel reorganization.

3.2 Braided Characteristics

The ABI curves (Fig. 4) generally follow oscillatory or polynomial-like trajectories rather than linear trends. Several segments display alternating periods of increasing and decreasing braiding intensity, suggesting cyclic adjustment between sediment deposition and channel consolidation. However, the long-term direction remains upward, implying gradual enhancement of channel instability and sediment-bar

development. The increasing ABI values indicate that exposed chars and sandbars became progressively more extensive through time, particularly after 2000. This may reflect increased sediment accumulation, enhanced channel bifurcation, or reduced flow confinement within certain reaches (Ashmore, 2013; Das & Islam, 2023).

Segment A maintained consistently high ABI values throughout the study period (mean = 0.514), indicating persistent multi-thread channel development and extensive bar formation associated with active braided morphology. In contrast, Segment B exhibited the greatest temporal variability (mean = 0.374), characterized by a pronounced increase during the 1990s, a sharp decline around 2004–2006, and subsequent recovery, reflecting repeated transitions between braided and semi-single-thread channel conditions driven by alternating channel consolidation and renewed bifurcation. Segment C showed a gradual but sustained increase in ABI (mean = 0.391), accompanied by widening of the active channel belt and increasing centerline divergence, suggesting progressive intensification of bar development and braided activity after 2000. Segment D recorded the highest average braided intensity (mean = 0.526) and the largest long-term increase, reaching an ABI of 0.715 by 2026, indicating extensive sediment accumulation, continuous channel bifurcation, and repeated reorganization of the active river corridor, making it one of the most morphodynamically unstable reaches. Conversely, Segment E exhibited comparatively moderate and less variable ABI values (mean = 0.385), suggesting that although episodic braided development occurred, the reach remained predominantly meander-dominated with relatively greater channel confinement. Overall, the segment-wise ABI patterns demonstrate a downstream shift from persistent braided expansion in Segments A and D to comparatively stable meandering conditions in Segment E, while Segments B and C represent transitional reaches where alternating sediment deposition, channel bifurcation, and flow concentration produced substantial temporal variability. Table 1 summarizes the meandering and braided morphometric.

Table 1
Sinuosity and Aerial Braided Index (ABI) values for the five geomorphological segments, summarizing changes in channel curvature and braided intensity.

Year	Sinuosity					ABI				
	A	B	C	D	E	A	B	C	D	E
1988	1.067	1.037	1.005	1.062	1.404	0.285	0.161	0.246	0.287	0.420
1990	1.132	1.083	1.064	1.059	1.681	0.259	0.324	0.249	0.325	0.276
1992	1.098	1.237	1.027	1.072	1.243	0.371	0.369	0.197	0.450	0.324
1994	1.076	1.287	1.059	1.107	1.350	0.443	0.494	0.334	0.513	0.371
1996	1.096	1.185	1.152	1.064	1.144	0.514	0.470	0.323	0.565	0.378
1998	1.061	1.146	1.153	1.084	1.122	0.473	0.445	0.276	0.501	0.371
2000	1.095	1.022	1.026	1.026	1.280	0.454	0.471	0.251	0.461	0.340
2001	1.114	1.019	1.019	1.015	1.152	0.485	0.502	0.270	0.485	0.327
2004	1.131	1.020	1.007	1.015	1.056	0.510	0.152	0.407	0.512	0.422
2006	1.084	1.018	1.007	1.036	1.062	0.570	0.080	0.397	0.533	0.418
2009	1.076	1.027	1.004	1.010	1.052	0.543	0.344	0.417	0.438	0.343
2010	1.083	1.046	1.005	1.002	1.046	0.592	0.377	0.481	0.498	0.374
2011	1.059	1.087	1.002	1.010	1.044	0.557	0.330	0.466	0.488	0.376
2015	1.040	1.114	1.004	1.070	1.082	0.600	0.442	0.543	0.565	0.446
2016	1.048	1.095	1.010	1.050	1.090	0.596	0.415	0.544	0.551	0.427
2018	1.059	1.178	1.036	1.086	1.099	0.606	0.385	0.526	0.594	0.416
2020	1.073	1.144	1.046	1.189	1.132	0.607	0.461	0.573	0.641	0.372
2022	1.091	1.172	1.196	1.200	1.259	0.590	0.409	0.467	0.699	0.427
2023	1.054	1.176	1.246	1.186	1.227	0.585	0.390	0.426	0.706	0.414
2026	1.101	1.041	1.186	1.230	1.372	0.645	0.454	0.435	0.715	0.452

3.3 Channel Migration Characteristics

The migration results (Fig. 5) indicate that leftward movement generally exhibited larger positive displacement magnitudes, while rightward migration displayed episodic extreme shifts. Several intervals show unusually high migration values, indicating localized avulsion or rapid channel relocation.

Segment A experienced the highest overall migration variability, with comparable mean leftward (1.18 km) and rightward (− 1.14 km) movements and several extreme displacements exceeding ± 8 km, indicating repeated channel relocation, intense bank erosion, and braided-channel instability driven by bar-induced

flow redistribution (Islam & Guchhait, 2024). Segment B exhibited comparatively balanced migration (1.16 km leftward and − 0.83 km rightward), characterized by alternating directional shifts around a relatively stable channel axis, suggesting oscillatory adjustment within a transitional braided–meandering system. Migration intensity decreased in Segment C (0.76 km leftward and − 0.57 km rightward), where channel movement was more gradual and systematic despite increasing sinuosity and braided intensity, indicating relatively constrained lateral adjustment. In contrast, Segment D displayed highly asymmetric migration, with moderate average leftward movement (0.84 km) but several extreme rightward displacements exceeding − 11 km, reflecting episodic channel avulsion, rapid relocation of the dominant flow path, and repeated reorganization of braided channels, making it one of the most morphodynamically unstable reaches. Segment E also exhibited substantial migration variability, particularly toward the right bank (mean = − 1.45 km), with major displacement events approaching − 9 km. Coupled with its high sinuosity variability, these migration patterns suggest recurrent meander expansion, bend migration, and cutoff processes. The results (Table 2) indicate that the upstream reaches (Segments A and B) are dominated by braided-channel redistribution and frequent lateral oscillation, the middle reach (Segment C) exhibits relatively stable and progressive adjustment, whereas the downstream reaches (Segments D and E) experience larger episodic channel shifts associated with avulsion and meander reorganization.

Table 2
Summary of channel migration distances (km) measured as leftward (LW) and rightward (RW) displacement for the five geomorphological segments of the Padma River.

Segment	**A**		**B**		**C**		**D**		**E**	
Year Dir.	LW	RW	LW	RW	LW	RW	LW	RW	LW	RW
1988-90	0.971	2.671	0.539	0.866	1.156	0.722	0.000	2.198	0.609	1.760
1990-92	0.754	1.356	1.359	2.437	0.956	0.098	0.847	1.272	0.209	5.169
1992-94	5.147	0.877	0.889	0.784	0.706	0.000	0.296	0.254	0.968	0.375
1994-96	0.373	1.996	0.687	1.689	1.012	0.368	0.129	0.513	0.000	2.710
1996-98	0.388	7.922	0.335	0.732	0.446	0.495	0.220	0.062	0.466	0.362
1998-00	0.628	0.559	6.354	0.000	2.033	0.760	10.430	0.000	8.918	0.077
2000-01	0.161	0.308	0.204	0.510	0.000	3.473	0.000	11.655	0.000	9.174
2001-04	0.622	0.500	0.345	0.293	0.230	0.636	0.322	0.000	0.006	1.393
2004-06	8.747	0.613	0.526	0.800	0.612	0.295	1.114	0.000	0.366	0.430
2006-09	0.861	0.609	0.182	0.822	0.333	0.168	1.417	0.589	0.977	0.337
2009-10	0.317	0.198	0.361	0.270	0.293	0.131	0.009	0.423	0.120	0.283
2010-11	0.239	0.428	0.546	0.396	0.251	0.042	0.060	0.276	0.211	0.141
2011-15	0.590	0.282	0.063	1.594	0.275	0.483	0.000	1.887	0.710	0.334
2015-16	0.192	0.255	0.073	0.305	0.334	0.094	0.113	0.115	0.109	0.133
2016-18	0.705	0.439	0.816	0.829	0.607	0.382	0.082	0.695	0.225	0.088
2018-20	0.204	0.531	0.038	0.609	0.771	0.091	0.551	0.242	0.503	0.012
2020-22	0.346	0.227	0.280	1.012	1.474	0.703	0.467	0.176	0.947	0.058
2022-23	0.164	0.415	0.365	0.184	0.348	0.259	0.171	0.128	0.367	0.348
2023-26	0.676	1.312	5.422	0.474	0.713	0.417	0.496	0.061	1.014	0.158
1988-26	1.557	1.370	3.823	1.916	2.553	1.757	0.073	5.152	0.926	5.565

4. Discussion: Long-term Morphodynamic Behavior of Padma River

The combined analysis of sinuosity, ABI, migration, centerlines, and river-plane evolution indicates that the Padma River exhibits long-term oscillatory morphodynamics characterized by alternating phases of meandering amplification, braided expansion, and channel reorganization (Fig. 6).

Several important relationships emerge from the results; (1) increasing ABI generally corresponds to enhanced channel instability and widening of the active river corridor, (2) high migration zones are

commonly associated with extensive braided development and repeated centerline divergence, (3) segments with strong sinuosity fluctuations often experienced periodic channel shortening or realignment, (4) the river does not behave uniformly; instead, each segment exhibits distinct morphodynamic responses depending on local flow distribution, sediment deposition, and channel geometry (Rashid & Habib, 2024; Raff et al., 2023).

The temporal behavior of the Padma River follows a quasi-cyclic morphodynamic system in which periods of intensified meandering are followed by increased braiding and channel redistribution. Temporal fluctuations observed in sinuosity and ABI curves reveal repeated phases of channel expansion, meander amplification, braided intensification, and subsequent reorganization throughout the 1988–2026 period. The sinuosity curves display broad oscillatory behavior with major peaks occurring during the early 1990s and again after 2010, suggesting an approximate recurrence interval between major phases of enhanced meandering. Similarly, ABI trends exhibit polynomial-like oscillation with increasing braided intensity following periods of elevated sinuosity, indicating a delayed geomorphological response between meander development and channel bifurcation. This lag relationship suggests that increased channel curvature initially promotes lateral erosion and sediment redistribution, which subsequently enhances bar formation and braided channel development. Several reaches, particularly Segments A, D, and E, show repeated reoccupation of previous channel zones, implying cyclical redistribution of flow and sediment within the active river corridor. Migration statistics also indicate clustering of major lateral adjustment events approximately every one to two decades, with alternating leftward and rightward displacement patterns. Collectively, these observations suggest that the Padma River undergoes a dominant morphodynamic oscillation cycle of approximately 12–18 years, superimposed by smaller sub-cycles of roughly 6–8 years associated with localized bar dynamics and short-term channel adjustments. The oscillatory behavior likely reflects the interaction between monsoonal discharge variability, sediment loading from the upstream Jamuna system, bar accretion, bank erosion, and channel avulsion processes. However, despite this cyclic tendency, the long-term increase in ABI across most segments indicates that the river may gradually be transitioning toward greater braided instability through time. It indicates that while the Padma River repeatedly returns to similar morphological states, the overall system is not in complete equilibrium and may be experiencing progressive long-term geomorphological transformation (Xia et al., 2021; Jarriel et al., 2020).

The ABI pattern likely reflects alternating phases of channel concentration and braided expansion. During periods of dominant single-thread flow, sediment transport capacity increases and portions of exposed bars become re-eroded, temporarily reducing ABI values. Conversely, during periods of reduced channel confinement, sediment deposition intensifies within the active corridor, promoting formation of mid-channel bars, chute channels, and multiple flow threads, thereby increasing ABI. However, despite these short-term fluctuations, the overall ABI trend increases consistently across most segments, indicating a gradual long-term enhancement of braided characteristics within the Padma system. This increase may be associated with sustained high sediment supply from the upstream Ganges–Jamuna system, increasing instability of channel banks, and repeated redistribution of sediments within the active valley corridor. Previous studies have shown that the GBM river system carries one of the largest sediment loads in the world, with

significant sediment influx derived from Himalayan erosion and monsoon-driven discharge variability (Islam et al., 2022).

Recent geomorphological investigations have also reported increasing bar development and channel widening within the Padma–Jamuna system due to excessive sediment deposition and unstable flow partitioning (Halder & Chowdhury, 2023). Therefore, the increasing ABI observed in this study likely indicates that sediment deposition and in-channel bar accretion are progressively exceeding the river's capacity for stable channel confinement. Simultaneously, higher erosion rates along outer banks continuously introduce additional sediment into the system, further enhancing braided development. Thus, the Padma River appears to be evolving toward a more laterally unstable and sediment-dominated morphodynamic condition, even though short-term oscillatory adjustments continue to occur within the broader long-term trend (Baki & Gan, 2012; Sarker et al., 2014)

5. Conclusion

The results demonstrate that the Padma River exhibits highly dynamic and spatially heterogeneous morphodynamic behavior characterized by continuous channel migration, braided expansion, meander adjustment, bar accretion, and repeated reorganization of the dominant flow pathway. Despite its contributions, the study has several limitations. First, the analysis relied primarily on planform morphometry and did not incorporate field-based sediment measurements, bathymetric surveys, or hydrodynamic modelling. Second, migration assessment was based on two-dimensional centerline displacement and therefore could not fully capture vertical channel adjustments or subsurface sediment processes. In addition, although NDWI-based classification effectively delineated water and exposed bars, some uncertainties may remain in distinguishing temporary floodplain inundation from active channel features. Future research should therefore incorporate LIDAR surveying, bathymetric data, sediment transport modelling, and hydrodynamic simulations to better understand the mechanisms driving the observed morphodynamic oscillations. Integration of discharge variability, monsoon intensity, and climate-related hydrological changes would further improve understanding of long-term river evolution within the Padma system. This reach-scale evidence is critical for delineating erosion-prone areas, focusing river training works, protecting infrastructure and ultimately for floodplain management. Hence, this study addresses both theoretical aspects of large alluvial river dynamics and practical considerations for a river corridor central to the economy and sustainability of Bangladesh.

Declarations

Ethics Approval

Not applicable

Consent to Participate

Not applicable

Consent to Publish

Not applicable

Declaration of Competing Interest

The authors declare none.

Authorship

As the corresponding author, I (Milon Bokshi) confirm on behalf of all co-authors that all authors listed have contributed significantly to the development, analysis, and writing of this manuscript, and meet the journal's criteria for authorship.

Funding

This research did not receive any specific grant from funding agencies in the public, commercial, or not-for-profit sectors.

Author Contribution

M.B. wrote the original draft, conceptualized and initialized the methodology. M.N.I. and M.M.M. reviewed, supervised, and edited the draft and M.J.H. reviewed and prepared the manuscript.

Acknowledgement

The authors sincerely acknowledge the United States Geological Survey (USGS) for providing free access to the Landsat satellite imagery used in this study through the Google Earth Engine (GEE) platform. Figure 2 is created using the assistance of ChatGPT 5.2.

Data Availability

All processed datasets generated and analyzed during this study, including codes, river centerlines, planes, segmented morphometric datasets, sinuosity measurements, Aerial Braided Index (ABI) values, migration statistics, and supplementary spatial outputs, are publicly available at https://doi.org/10.5281/zenodo.21644077. The Landsat satellite imagery utilized in this study was obtained from the United States Geological Survey (USGS) archive through the Google Earth Engine platform.

References

1. Arefin, R., Meshram, S. G., & Seker, D. Z. (2021). River channel migration and land-use/land-cover change for Padma River at Bangladesh: a RS-and GIS-based approach. International Journal of Environmental Science and Technology, 18(10), 3109–3126. https://doi.org/10.1007/s13762-020-03063-7
2. Ashmore, P. (2013), 9.17 Morphology and dynamics of braided rivers. In *Elsevier eBooks* (pp. 289–312). https://doi.org/10.1016/b978-0-12-374739-6.00242-6
3. Baki, A. B. M., & Gan, T. Y. (2012). Riverbank migration and island dynamics of the braided Jamuna River of the Ganges–Brahmaputra basin using multi-temporal Landsat images. *Quaternary International*, *263*, 148–161. https://doi.org/10.1016/j.quaint.2012.03.016
4. Boothroyd, R. J., Nones, M., & Guerrero, M. (2021). Deriving planform morphology and vegetation coverage from remote sensing to support river management applications. Frontiers in Environmental Science, 9, 657354. https://doi.org/10.3389/fenvs.2021.657354
5. Bristow, C. S., & Best, J. L. (1993). Braided rivers: perspectives and problems. *Geological society, London, special publications*, *75*(1), 1–11. https://doi.org/10.1144/GSL.SP.1993.075.01.01
6. Chakraborty, K., & Saha, S. (2022). Assessment of bank erosion and its impact on land use and land cover dynamics of Mahananda River basin (Upper) in the Sub-Himalayan North Bengal, India. SN Applied Sciences, 4(1), 20. https://doi.org/10.1007/s42452-021-04904-x
7. Das, B. C., & Islam, A. (2023). Reviewing braiding indices of the river channel in an attempt to establish alternatives. MethodsX, 10, 102042. https://doi.org/10.1016/j.mex.2023.102042
8. Dewan, A., Corner, R., Saleem, A., Rahman, M. M., Haider, M. R., Rahman, M. M., & Sarker, M. H. (2017). Assessing channel changes of the Ganges-Padma River system in Bangladesh using Landsat and hydrological data. Geomorphology, 276, 257–279. https://doi.org/10.1016/j.geomorph.2016.10.017
9. Du, Y., Zhang, Y., Ling, F., Wang, Q., Li, W., & Li, X. (2016). Water bodies' mapping from Sentinel-2 imagery with modified normalized difference water index at 10-m spatial resolution produced by sharpening the SWIR band. *Remote Sensing*, *8*(4), 354. https://doi.org/10.3390/rs8040354
10. Goodbred Jr, S. L., & Kuehl, S. A. (2000). Enormous Ganges-Brahmaputra sediment discharge during strengthened early Holocene monsoon. *Geology*, *28*(12), 1083–1086. https://doi.org/10.1130/0091-7613(2000)28%3C1083:EGSDDS%3E2.0.CO;2
11. Halder, A., & Mowla Chowdhury, R. (2023). Evaluation of the river Padma morphological transition in the central Bangladesh using GIS and remote sensing techniques. International Journal of River Basin Management, 21(1), 21–35. https://doi.org/10.1080/15715124.2021.1879095
12. Hong, Z., Ling, F., Yang, Q., Mapfumo, P., Wang, Z., Wang, L., … Yan, X. (2026). Integrating planet binary maps and Landsat fraction series for national surface water monitoring: a case study in Zimbabwe, Africa. *International Journal of Digital Earth*, *19*(2), 2696675. https://doi.org/10.1080/17538947.2026.2696675
13. Hu, J., Xia, J., & Deng, S. (2025). Analysis of planform migration characteristics and lag effects in meandering rivers using remote sensing image interpretation. *Science China Earth Sciences*, *68*(3),

824–835. https://doi.org/10.1007/s11430-024-1483-7

14. Islam, A. R. M. T., Talukdar, S., Akhter, S., Eibek, K. U., Rahman, M. M., Pal, S., … Mosavi, A. (2022). Assessing the impact of the Farakka Barrage on hydrological alteration in the Padma River with future insight. *Sustainability*, *14*(9), 5233. https://doi.org/10.3390/su14095233
15. Islam, A., & Guchhait, S. K. (2024). Riverbank erosion: basic concepts and approaches. In *Riverbank erosion in the Bengal delta: An integrated perspective* (pp. 3–22). Cham: Springer International Publishing. https://doi.org/10.1007/978-3-031-47010-3_1
16. Islam, M. R., Begum, S. F., Yamaguchi, Y., & Ogawa, K. (1999). The Ganges and Brahmaputra rivers in Bangladesh: basin denudation and sedimentation. Hydrological Processes, 13(17), 2907–2923. https://doi.org/10.1002/(SICI)1099-1085(19991215)13:17%3C2907::AID-HYP906%3E3.0.CO;2-E
17. Jarriel, T., Isikdogan, L. F., Bovik, A., & Passalacqua, P. (2020). System wide channel network analysis reveals hotspots of morphological change in anthropogenically modified regions of the Ganges Delta. Scientific Reports, 10(1), 12823. https://doi.org/10.1038/s41598-020-69688-3
18. Li, J., Donselaar, M. E., Aria, S. E. H., Koenders, R., & Oyen, A. M. (2014). Landsat imagery-based visualization of the geomorphological development at the terminus of a dryland river system. *Quaternary International*, *352*, 100–110. https://doi.org/10.1016/j.quaint.2014.06.041
19. Li, J., Xia, J., Kong, L., Ji, Q., & Li, L. (2024). Geomorphic adjustments of channel bars in the braided reach of the lower Yellow river from 1986 to 2018. Catena, 236, 107735. https://doi.org/10.1016/j.catena.2023.107735
20. Marcus, W. A., & Fonstad, M. A. (2008). Optical remote mapping of rivers at sub-meter resolutions and watershed extents. Earth Surface Processes and Landforms: The Journal of the British Geomorphological Research Group, 33(1), 4–24. https://doi.org/10.1002/esp.1637
21. McFeeters, S. K. (1996). The use of the Normalized Difference Water Index (NDWI) in the delineation of open water features. International journal of remote sensing, 17(7), 1425–1432. https://doi.org/10.1080/01431169608948714
22. Miah, M. D., Chowdhury, N. A., & Ali, Y. (2025). Monitoring multi-decadal riverbank dynamics of the Padma river in Bangladesh using geospatial analysis and DSAS model. Discover Geoscience, 3(1), 238. https://doi.org/10.1007/s44288-025-00353-w
23. Ophra, S. J., Begum, S., Islam, R., & Islam, M. N. (2018). Assessment of bank erosion and channel shifting of Padma River in Bangladesh using RS and GIS techniques. Spatial Information Research, 26(6), 599–605. https://doi.org/10.1007/s41324-018-0202-2
24. Preota, S. A., Joy, M. F. R., Rahman, M. M., Mia, M. B., Karim, S., & Amin, G. M. R. (2026). Quantitative Hydro-morphological Analysis of the Ganges-Padma River System in Bangladesh. Global and Earth Surface Processes Change, 100016. https://doi.org/10.1016/j.gespch.2026.100016
25. Raff, J. L., Goodbred, S. L., Pickering, J. L., Sincavage, R. S., Ayers, J. C., Hossain, M. S., … Williams, L. A. (2023). Sediment delivery to sustain the Ganges-Brahmaputra delta under climate change and anthropogenic impacts. Nature communications, 14(1). https://doi.org/10.1038/s41467-023-38057-9
26. Rahman, M., Dustegir, M., Karim, R., Haque, A., Nicholls, R. J., Darby, S. E., … Akter, M. (2018). Recent sediment flux to the Ganges-Brahmaputra-Meghna delta system. Science of the total environment, 643,

1054–1064. https://doi.org/10.1016/j.scitotenv.2018.06.147

27. Rashid, M. B., & Habib, M. A. (2024). Channel bar development, braiding and bankline migration of the Brahmaputra-Jamuna river, Bangladesh through RS and GIS techniques. International Journal of River Basin Management, 22(2), 203–215. https://doi.org/10.1080/15715124.2022.2118281
28. Sarker, M. H., Thorne, C. R., Aktar, M. N., & Ferdous, M. R. (2014). Morpho-dynamics of the Brahmaputra–Jamuna river, Bangladesh. Geomorphology, 215, 45–59. https://doi.org/10.1016/j.geomorph.2013.07.025
29. Schumm, S. A. (1985). Patterns of alluvial rivers. *Annual Review of Earth and Planetary Sciences, Vol. 13, p. 5*, *13*, 5. https://doi.org/10.1146/annurev.ea.13.050185.000253
30. Wahiduzzaman, M., & Yeasmin, A. (2022). An observation of the changing trends of a river channel pattern in Bangladesh using satellite images. Applied Sciences, 12(22), 11604. https://doi.org/10.3390/app122211604
31. Wolman, M. G., & Leopold, L. B. (1957). *River flood plains: some observations on their formation* (Vol. 282, pp. 87–109). Washington, DC: US Government Printing Office.
32. Xia, J., Wang, Y., Zhou, M., Deng, S., Li, Z., Wang, Z., … Li, J. (2021). Variations in channel centerline migration rate and intensity of a braided reach in the lower yellow river. Remote Sensing, 13(9). https://doi.org/10.3390/rs13091680
33. Yang, C., Cai, X., Wang, X., Yan, R., Zhang, T., Zhang, Q., & Lu, X. (2015). Remotely sensed trajectory analysis of channel migration in Lower Jingjiang Reach during the period of 1983–2013. Remote Sensing, 7(12), 16241–16256. https://doi.org/10.3390/rs71215828
34. Zaman, M. A., Niha, F. T., Shimla, U. S., Sifa, S. F., & Rahman, M. M. (2026). Multi-temporal assessment of river morphological changes using earth observation techniques in Dumuria Upazila of Khulna district, Bangladesh. *Environmental Challenges*, 101452. https://doi.org/10.1016/j.envc.2026.101452
35. Zhang, X., Liu, L., Chen, X., Gao, Y., Xie, S., & Mi, J. (2021). GLC_FCS30: Global land-cover product with fine classification system at 30 m using time-series Landsat imagery. Earth System Science Data, 13(6), 2753–2776. https://doi.org/10.5194/essd-13-2753-2021
36. Zhao, S. H., Zhang, C. M., Zhang, X. H., & Liu, J. L. (2026). A novel method for automatic river channel morphology extraction from remote sensing satellite images: A case study of the Golmud fluvial fan. *China Geology*, *9*(2), 333–348. https://doi.org/10.31035/cg2025057

Figures

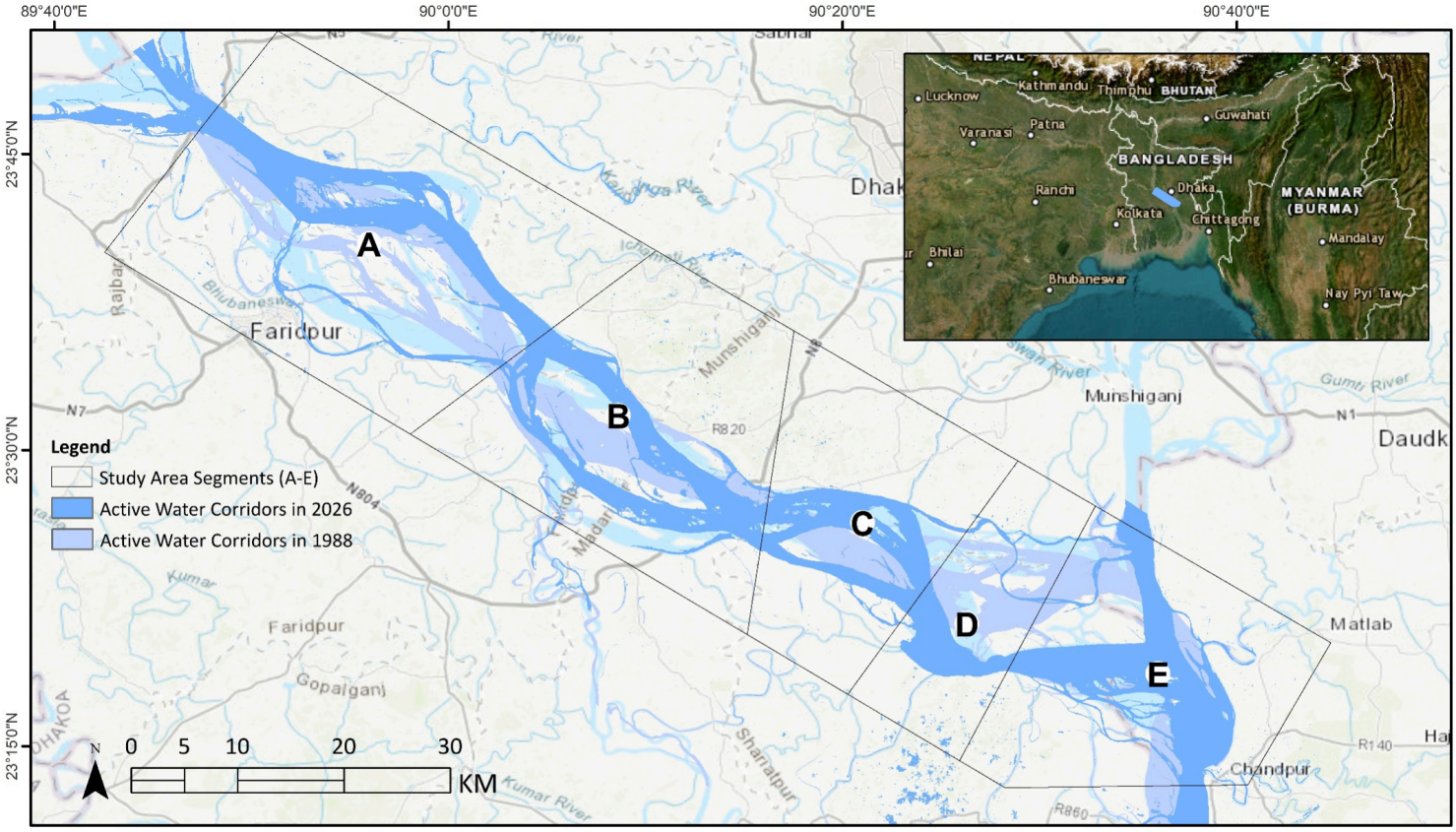


Figure 1

Study area of the Padma River investigated in this research, extending from the Jamuna–Padma confluence near Paturia to Chandpur Puran Bazar, where the Padma joins the Meghna River. The approximately 105 km river reach was subdivided into five geomorphologically distinct segments (A–E) based on channel curvature, bend transition, and historical centerline density.

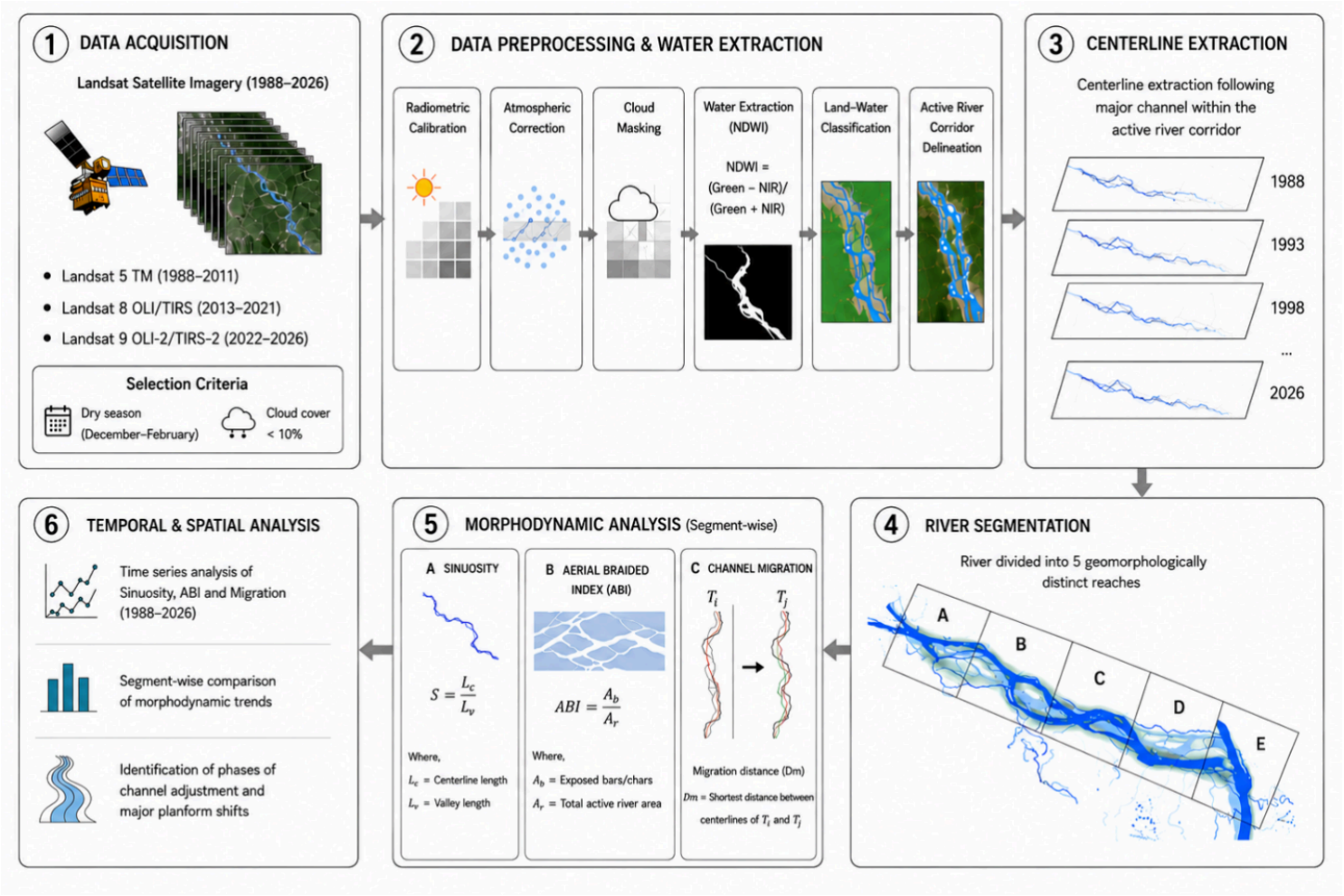


Figure 2

Methodological framework adopted for the long-term morphodynamic analysis of the Padma River (1988–2026) using multi-temporal Landsat imagery.

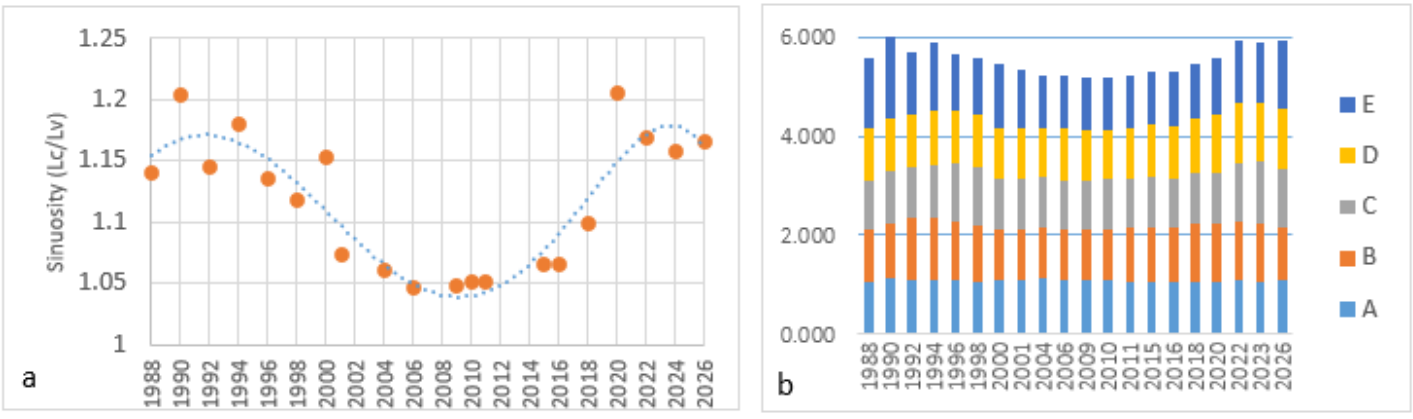


Figure 3

Sinuosity of the Padma River; (a) the overall sinuosity along the entire 105 km study reach from Paturia to Chandpur during 1988–2026; (b) Segment-wise sinuosity for the five geomorphological reaches (Segments

A–E) over the same study period.

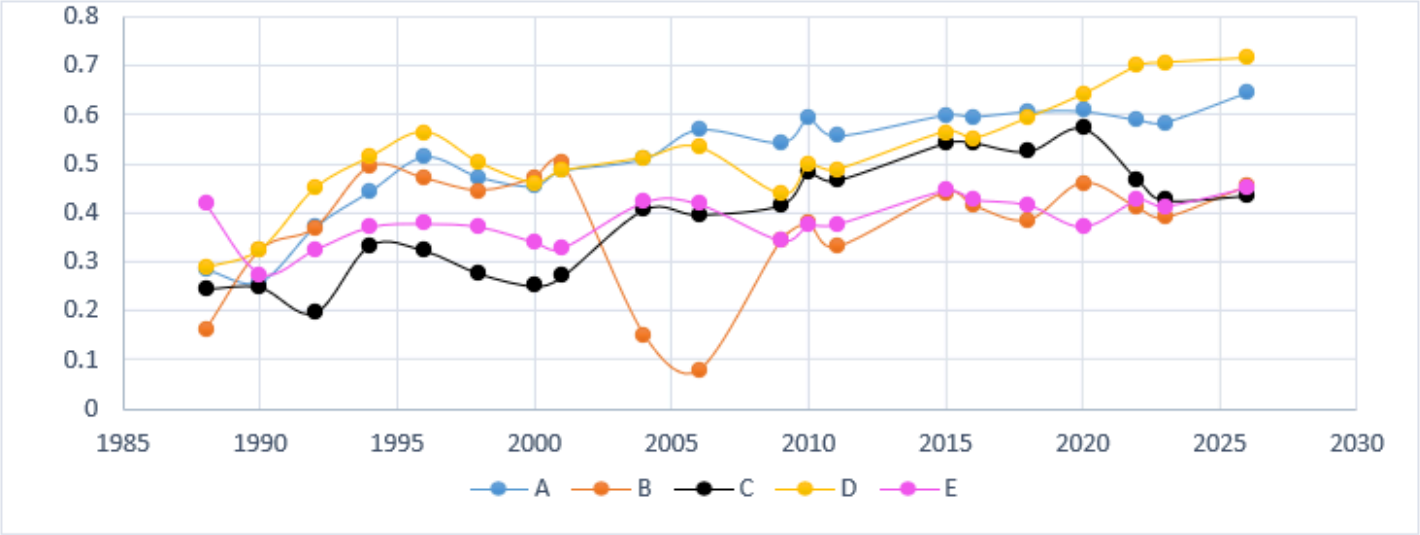


Figure 4

ABI values for the five geomorphological segments (A–E) illustrate distinct spatial and temporal patterns of braided-channel development. Segments Aand Dexhibit a persistent long-term increase in braided intensity, whereas Segment Bshows the largest temporal variability. Segment C demonstrates a gradual increase after 2000, while Segment E maintains comparatively stable values.

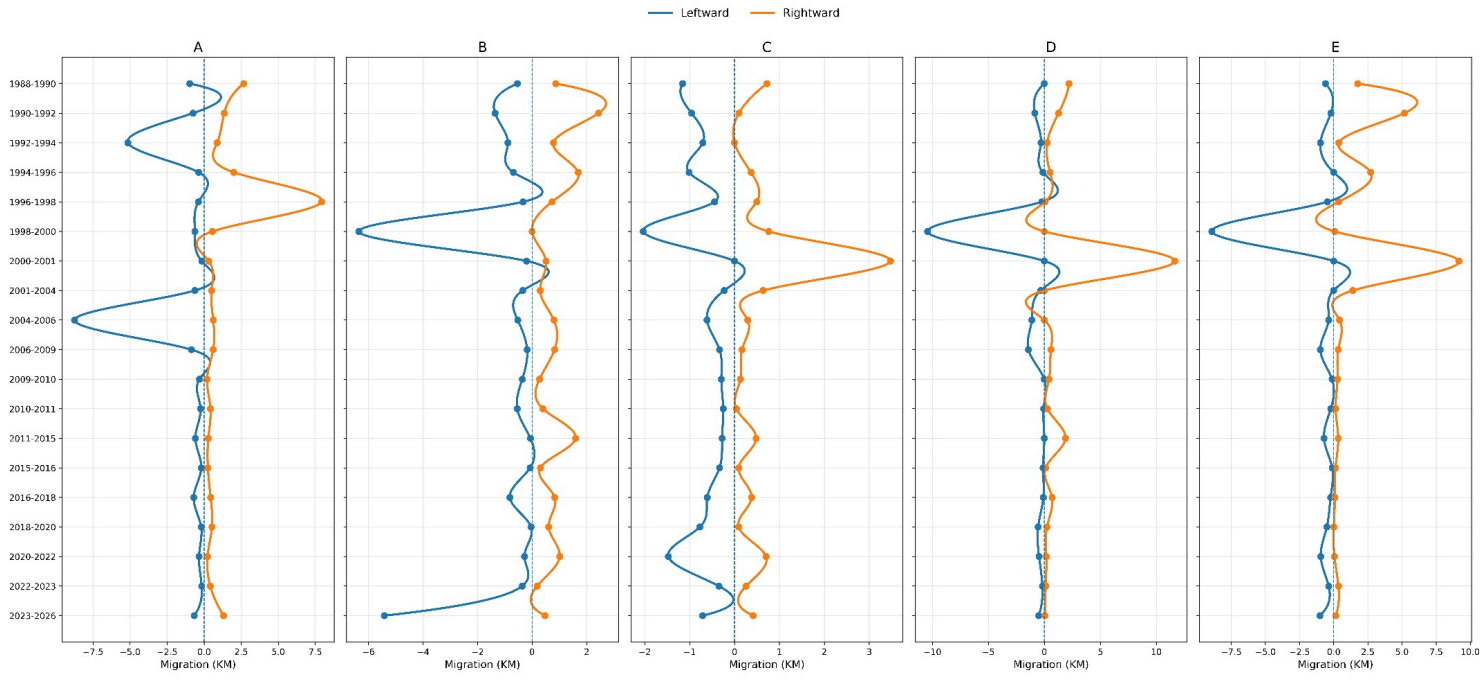


Figure 5

Leftward and rightward channel migration measured in KM along the five geomorphological segments (A–E) of the Padma River. Positive values represent left-bank migration, whereas negative values indicate right-

bank migration, highlighting differences in the magnitude, direction, and asymmetry of lateral channel adjustment among the river segments.

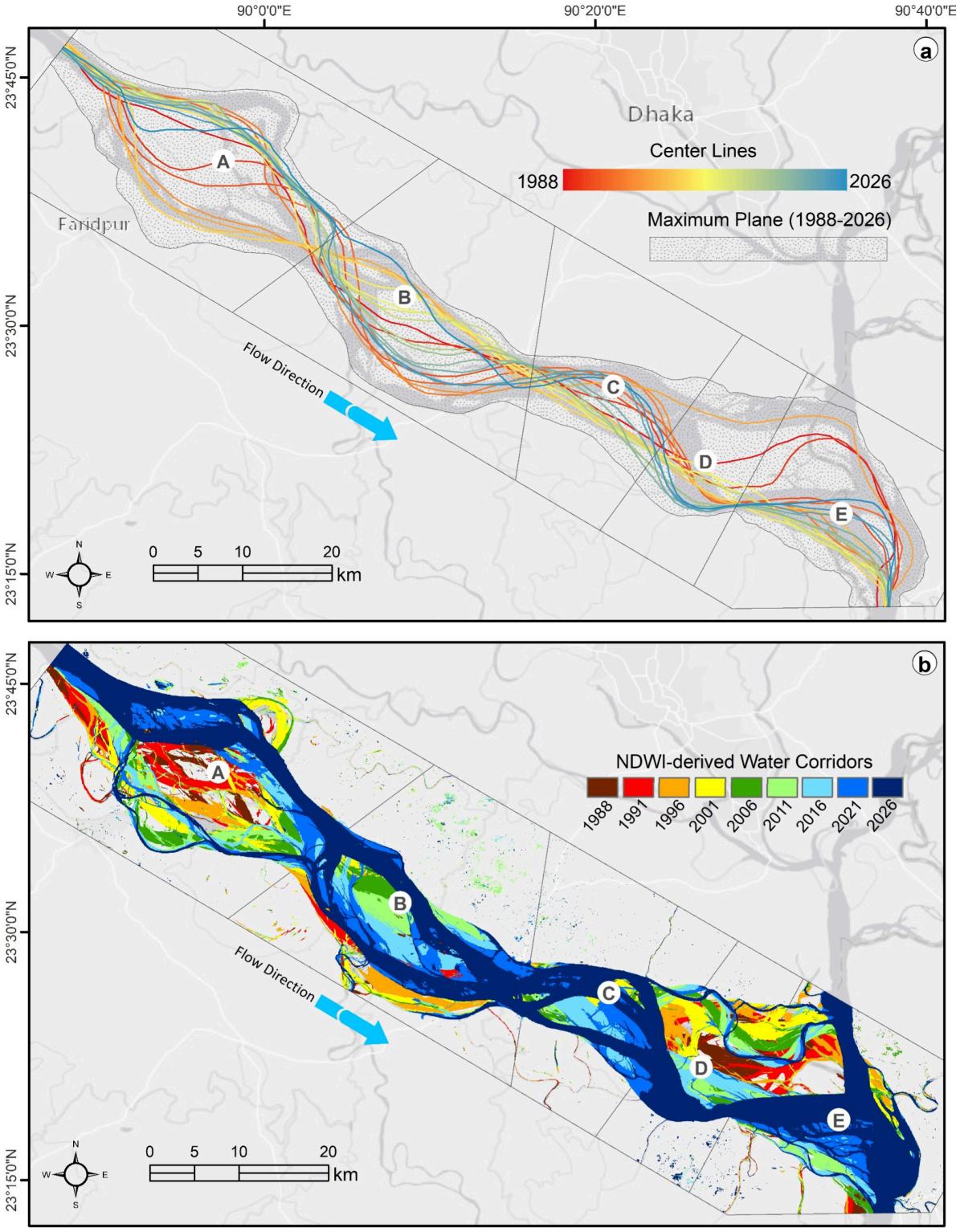


Figure 6

Long-term morphodynamic behavior of the Padma River. (a)Extracted river centerlines overlaid on the maximum active river plane; (b) Representative NDWI-derived water corridors selected at approximately

five-year intervals, illustrating the progressive evolution of the active channel over the period across the study reach.